International Journal of Nanomedicine

Dovepress
open access to scientific and medical research

Open Access Full Text Article

ORIGINAL RESEARCH

Application of magnetically induced hyperthermia in the model protozoan *Crithidia fasciculata* as a potential therapy against parasitic infections

This article was published in the following Dove Press journal:
International Journal of Nanomedicine
5 October 2012
Number of times this article has been viewed

V Grazú[1]
AM Silber[2]
M Moros[1]
L Asín[1]
TE Torres[1,3,5]
C Marquina[3,4]
MR Ibarra[1,3]
GF Goya[1,3]

[1]Instituto de Nanociencia de Aragón (INA), Universidad de Zaragoza, Zaragoza, Spain; [2]Departamento de Parasitologia, Instituto de Ciências Biomédicas, Universidade de São Paulo, São Paulo, Brazil; [3]Departamento de Física de la Materia Condensada, Facultad de Ciencias, Universidad de Zaragoza, Zaragoza, Spain; [4]Instituto de Ciencia de Materiales de Aragón (ICMA), CSIC, Universidad de Zaragoza, Zaragoza, Spain; [5]Laboratorio de Microscopías Avanzadas (LMA), Universidad de Zaragoza, Zaragoza, Spain

Background: Magnetic hyperthermia is currently a clinical therapy approved in the European Union for treatment of tumor cells, and uses magnetic nanoparticles (MNPs) under time-varying magnetic fields (TVMFs). The same basic principle seems promising against trypanosomatids causing Chagas disease and sleeping sickness, given that the therapeutic drugs available have severe side effects and that there are drug-resistant strains. However, no applications of this strategy against protozoan-induced diseases have been reported so far. In the present study, *Crithidia fasciculata*, a widely used model for therapeutic strategies against pathogenic trypanosomatids, was targeted with Fe_3O_4 MNPs in order to provoke cell death remotely using TVMFs.

Methods: Iron oxide MNPs with average diameters of approximately 30 nm were synthesized by precipitation of $FeSO_4$ in basic medium. The MNPs were added to *C. fasciculata* choanomastigotes in the exponential phase and incubated overnight, removing excess MNPs using a DEAE-cellulose resin column. The amount of MNPs uploaded per cell was determined by magnetic measurement. The cells bearing MNPs were submitted to TVMFs using a homemade AC field applicator (f = 249 kHz, H = 13 kA/m), and the temperature variation during the experiments was measured. Scanning electron microscopy was used to assess morphological changes after the TVMF experiments. Cell viability was analyzed using an MTT colorimetric assay and flow cytometry.

Results: MNPs were incorporated into the cells, with no noticeable cytotoxicity. When a TVMF was applied to cells bearing MNPs, massive cell death was induced via a nonapoptotic mechanism. No effects were observed by applying TVMF to control cells not loaded with MNPs. No macroscopic rise in temperature was observed in the extracellular medium during the experiments.

Conclusion: As a proof of principle, these data indicate that intracellular hyperthermia is a suitable technology to induce death of protozoan parasites bearing MNPs. These findings expand the possibilities for new therapeutic strategies combating parasitic infection.

Keywords: magnetic hyperthermia, magnetic nanoparticles, trypanosomatids, *Crithidia fasciculata*

Introduction

Diseases caused by the *Trypanosoma* and *Leishmania* genera affect a global population of at least 20 million people, with an estimated at-risk population of approximately 450 million people.[1,2] These statistics indicate that trypanosomatid-induced diseases are a severe sanitary problem, with the resulting disease burden affecting much of the population residing in the tropical and subtropical regions of the globe.[3,4] Despite the sanitary relevance of trypanosomatid-induced diseases to human health, no satisfactory

Correspondence: Gerardo F Goya
Instituto de Nanociencia de Aragón, Universidad de Zaragoza, Calle Mariano Esquillor s/n Campus Rio Ebro, 50018 Zaragoza, Spain
Tel +348 7655 5362
Fax +349 7676 2776
Email goya@unizar.es

treatments exist to combat these infections.[5–7] The two therapeutic agents that are presently in use for the treatment of Chagas disease are nifurtimox and benzimidazole; however, these drugs were developed approximately 40 years ago.[8] The main disadvantages of these treatments are a high level of toxicity and low therapeutic efficiency during the chronic phase of the disease. The latter disadvantage is a serious problem because Chagas disease is often diagnosed during the chronic phase; therefore, the majority of infected people miss the opportunity to be treated using effective chemotherapy.[9] In addition, several cases of drug-resistant or partially resistant strains have been reported for both of these drugs.[10]

The initial stages of *Trypanosoma brucei* infections, when the central nervous system is not compromised, can be treated using suramin or pentamidine.[11] Again, these drugs are not effective during the late stages of the disease (when the majority of cases are diagnosed) because they do not traverse the blood–brain barrier. The first-line treatment for these cases is melarsoprol, which can cross the blood–brain barrier. Melarsoprol is a highly toxic drug that causes a myriad of serious side effects, including reactive encephalopathy, in approximately 20% of patients receiving this treatment.[12] For the treatment of diseases caused by *Leishmania* spp., pentavalent antimonials are used most often.[13] Although these drugs are effective for treating the cutaneous form of the disease, treatments for the parenteral form are limited. In addition, these drugs are highly toxic.

Amphotericin B and pentamidine are considered to be second-line drugs because of their serious and/or irreversible toxic effects. However, these drugs are now being reconsidered on the basis of new formulations or dosage regimens.[13–15] The fact that the majority of drugs currently used for trypanosomatid-induced diseases were developed approximately 40 years ago reflects the limited success of strategies to develop novel therapeutic treatments. This lack of success highlights the necessity for new strategies and tools to address this important public health issue.

Magnetic hyperthermia is a relatively new medical protocol[16] that uses magnetic nanoparticles (MNPs) to heat areas of the body by application of time-varying magnetic fields (TVMFs). The physical mechanisms underlying energy absorption by MNPs are related to magnetic relaxation of single domains by Arrhenius-Néel processes.[4,17] With the advent of nanotechnology, it has become possible to engineer efficient MNPs with the ability to absorb large amounts of energy from TVMFs (up to several kW per gram of material) to induce a local rise in temperature.[18] Because of their size, these nanoparticles can be incorporated into target cells, making it possible to heat small foci at the single cell level.[19] Application of hyperthermia using MNPs, alone or in combination with other therapeutic strategies, was proposed more than a decade ago as a therapeutic technique to treat cancer.[16] In the present study, we used *Crithidia fasciculata*, a nonpathogenic trypanosomatid and a well accepted model of other pathogenic trypanosomatid parasites,[20] to evaluate the use of magnetic hyperthermia as a potential trypanocidal treatment. The mechanisms of cell death and application of the principles of magnetic hyperthermia to treat parasitic diseases are discussed in later sections of this paper.

Materials and methods

Reagents and culture media

The chemicals and fetal calf serum used for the present study were purchased from Sigma (St Louis, MO). The other components of the culture medium were purchased from Difco (Lawrence, KS). The apoptosis detection kit was purchased from Immunostep (Coimbra, Portugal). The diethylaminoethyl (DEAE) cellulose (DE52) was purchased from Whatman (Dassel, Germany).

Cells

C. fasciculata choanomastigotes were grown at 28°C in Warren culture medium (brain heart infusion 37 g/L, hemin 100 ng/L, folic acid 100 mg/L) supplemented with 10% fetal calf serum. The cells were seeded in 75 cm^3 tissue culture plates at 1×10^6 cells/mL. *C. fasciculata* cultures were incubated until they reached the exponential phase (after approximately 24 hours of incubation). Using daily subculturing, the cells were maintained in the exponential growth phase for use in the studies. Cell counting was performed in a Neubauer chamber. The cells were evaluated for viability by optical microscopic observation of flagellar motility and by counting the number of viable cells after incubation with 2% Trypan blue in phosphate-buffered solution.

Magnetic nanoparticles

The MNPs used in the present study were synthesized using precipitation of iron (II) salt ($FeSO_4$) in the presence of a base (NaOH) and a mild oxidant (KNO_3) under a nitrogen atmosphere, as previously described in the literature.[21] Mixing the reactants over a 24-hour period resulted in Fe_3O_4 particles with average diameters of about 30 nm and colloidal stability in aqueous medium at pH 7.

Cell uptake of MNPs and separation of nonincorporated MNPs

The cells collected during the exponential growth phase were centrifuged and resuspended in fresh culture medium, adjusting concentrations to 2.5×10^8 cells/mL. The MNPs were added to a final concentration of 0.425 mg/mL and incubated at 28°C overnight with gentle agitation. To separate the cells from the nonincorporated MNPs, we took advantage of the fact that MNPs (isoelectric point 5.0) adsorb to DEAE-cellulose resin at pH 7.0 (isoelectric point 2.5), whereas *C. fasciculata* does not interact with the resin under these conditions. Briefly, the cells were washed twice with phosphate-buffered solution, resuspended in 12 mL of 2% glucose in phosphate-buffered solution, and incubated with 6 g DEAE-cellulose ionic exchange resin that was previously equilibrated with glucose in phosphate-buffered solution for 10 minutes with gentle agitation at room temperature. The cells were recovered with an efficiency of more than 95%.

Determination of cell-incorporated MNPs by magnetization measurements

The amounts of cell-associated MNPs were determined by measuring the saturation magnetization using a superconducting quantum interference device (MPMS-7T, Quantum Design, San Diego, CA). The magnetization measurements were conducted on dried MNPs or lyophilized MNP-loaded cells, and were performed as a function of the applied magnetic field up to 5 kOe (0.4 MA/m) at different temperatures between 5 K and 300 K.

Time-varying magnetic field application experiments

Aliquots of MNPs (10 mg/mL) or MNP-bearing cells (1.7×10^9 cells/mL) were submitted to alternating magnetic fields using a homemade AC field applicator. The magnetic field applicator, consisting of a resonant LC tank working close to the resonant frequency, was used to measure the specific power absorption of the samples. A magnetic field (f = 249 kHz, H = 13 kA/m) was achieved inside a gap of four (2 + 2) turns of a copper tube around high permeability polar pieces. The specific power absorption values were obtained from adiabatic measurements inside an insulated Dewar flask. The temperature data were measured using a fiberoptic temperature probe (Reflex™, Neoptix, Fairport, NY) that was immune to the radiofrequency environment. Prior to each experiment, temperature evolution was measured between the 5-minute and 10-minute time points, with the RF source turned off to establish a temperature baseline. Next, the power was turned on, and the temperature rise was monitored for a 30-minute period.

Scanning electron microscopy

Cells in the exponential growth phase were fixed with 2.5% glutaraldehyde in 0.1 M sodium cacodylate and 3% sucrose solution for 90 minutes at 4°C. The dehydration process was conducted by incubating the cells in increasing concentrations of methanol at 30%, 50%, 70%, and 100%. Each of these concentrations were used for 5 minutes in duplicate, and a final step was conducted using anhydride methanol for 10 minutes. A drop of the dehydrated cells in suspension was placed over a coverslip. Next, when the methanol was evaporated, the coverslip was coated with gold. The samples were then observed using scanning electron microscopy (EDX Hitachi S-3400 N, Instituto Carboquimica, Zaragoza, Spain). Secondary electron images were also performed.

Viability analysis

MTT assay

Cell viability was analyzed using the MTT colorimetric assay. For the cytotoxicity assay, 5×10^6 cells ($MNPs^-/TVMF^-$, $MNPs^-/TVMF^+$, $MNPs^+/TVMF^-$, or $MNPs^+/TVMF^+$) were resuspended in 100 µL of Warren culture medium. Next, 40 µL of MTT dye solution (5 mg/mL in glucose in phosphate-buffered solution) was added to each aliquot. After 4 hours of incubation in Eppendorf tubes at 28°C, the formazan crystals were dissolved by addition of 10% sodium dodecyl sulfate 100 µL. All of the cell debris, which has been shown to interfere with the assay, was removed by centrifugation (10 minutes at 13,000 × g). Next, absorbance of each supernatant was read using a microplate reader (Biotek ELX800, Winooski, VT) at 570 nm. The spectrophotometer was calibrated to zero absorbance using a culture medium without cells. The relative cell viability (%) compared with the control cells (the exponential-phase cells not submitted to any treatment) was calculated as [absorbance] test/[absorbance] control × 100. Each measurement was repeated at least five times to obtain mean values with standard deviations.

Flow cytometry

The cell viability was also measured using flow cytometry with a commercial apoptosis detection kit purchased from Immunostep. Briefly, 1×10^6 cells from each sample were resuspended in annexin-binding buffer, stained with 5 µL of annexin and 5 µL of propidium iodide, and incubated for 15 minutes at room temperature in the dark. The cell analysis

was performed using the FACSAria cytometer (Becton Dickinson, Franklin Lakes, NJ) and FACSDiva software.

Results and discussion

The magnetic and physicochemical properties of the MNPs used in the present study have been reported elsewhere.[22] The magnetic colloids were composed of cubic Fe_3O_4 nanoparticles with an average diameter of 30 ± 8 nm and saturation magnetization at room temperature of 85 emu/g, which is close to that of the bulk magnetite magnetization.[23] This synthesis route resulted in magnetic colloids with an isoelectric point of 5.0, electrostatically stabilized due to adsorption of SO_4^{2-} groups on the particle surface. The ability to dissipate heat under a TVMF of any type of MNP is measured by the specific power absorption given in watts per gram of magnetic material, which for the present MNPs and experimental conditions (f = 249 kHz, H = 13 kA/m) was found to be 83.6 W/g,[22] comparable with other specific power absorption values reported in the literature for Fe_3O_4 particles of similar size.[24–26] The selection of MNPs was made based on the known dependence of specific power absorption values on an average particle size and size distribution. Indeed, the strong dependence of the Nèel relaxation-based model on particle size yields a maximum value of specific power absorption for magnetite MNPs within a narrow range of diameters around 15–30 nm,[4] as experimentally confirmed in many colloidal system yields.[3,19,21] The precise value for this maximum will depend on other magnetic properties of the MNPs, such as magnetic anisotropy and saturation magnetization.

The optimal experimental conditions for *C. fasciculata* to incorporate MNPs were determined by a series of experiments as a function of incubation time, incubating *C. fasciculata* with a fixed MNP concentration for increasing times from 15 to 240 minutes. After incubation, the nonincorporated MNPs were separated by the column method detailed in the Materials and Methods section. The mass of magnetic material incorporated per cell was determined by measuring the saturation magnetization of 100 µL of culture medium containing about 10^9 cells and comparing these values with the magnetization of pure colloid.[27] From these data and the average particle size, the average number of MNPs incorporated per cell was calculated (Table 1). The number of MNPs incorporated decreased from a maximum of approximately 10^8 nanoparticles per cell after 15 minutes of incubation to approximately 10^6 nanoparticles per cell after 1 hour of incubation. Shorter incubation times resulted in low and highly variable cell charging, possibly due to the fact that the cells require an induction time to activate biological mechanisms to incorporate the MNPs. The time course of this decrease in cell-associated MNPs followed an exponential decay (R^2 0.9998), reaching a near-steady state after approximately 1 hour of incubation, which remained essentially constant for up to 12 hours of incubation (Figure 1 and Figure S1). From these experiments, we established 15 minutes of incubation as being the optimal condition for charging the cells with a reproducible and defined number of MNPs per cell.

To evaluate the suitability of MNPs for hyperthermic applications, it was necessary to assess the influence of these nanoparticles on cell viability and on incorporation and separation conditions. It was observed that, when compared with cells in the exponential phase, the nanoparticle-treated or mock-treated cultures submitted to separation conditions (incubated with DEAE-cellulose resin in glucose in phosphate-buffered solution) remained more than 95% viable (data not shown). This finding illustrates that the cell death observed in subsequent experiments was not due to previous exposure of the cells to toxic conditions.

Hyperthermia experiments

After the best conditions for maximum uptake of MNPs by the cells were determined (15 minutes of incubation, as stated above), the hyperthermia experiments were performed. The experiments were designed in a 2 × 2 row-column format (Figure 2), in which the four groups were defined as follows: cells not-bearing MNPs that were not submitted to TVMFs ($MNPs^-/TVMF^-$); cells bearing MNPs that were not submitted to magnetic field application ($MNPs^+/TVMF^-$); cells not bearing MNPs that were submitted to magnetic field application ($MNPs^-/TVMF^+$); and cells bearing MNPs that were submitted to magnetic field application ($MNPs^+/TVMF^+$).

Table 1 Average number of magnetic nanoparticles incorporated within a single cell as a function of incubation time, as calculated from the saturation magnetization of magnetically loaded cells

Time	15 minutes	30 minutes	45 minutes	1 hour	1.5 hours	2 hours	4 hours	12 hours
Mass of Fe_3O_4 (pg/cell)	12.3	0.55	0.31	0.14	0.22	0.15	0.23	0.18
Number of MNPs ($\times 10^6$)/cell	87	3.9	2.2	1.0	1.6	1.1	1.6	1.3

Abbreviation: MNPs, magnetic nanoparticles.

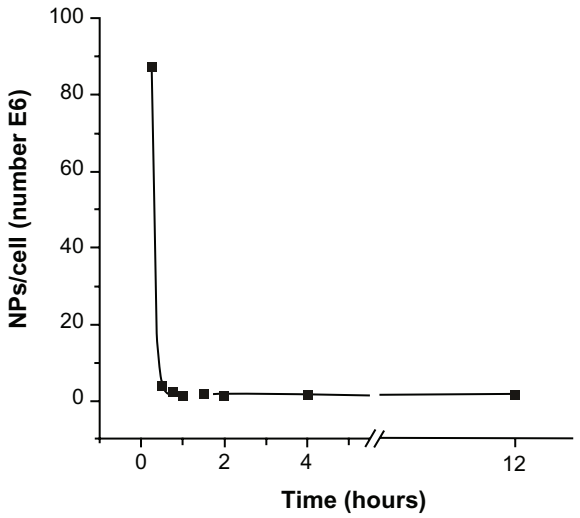

Figure 1 Number of magnetic nanoparticles uploaded per cell as a function of incubation time.
Notes: The observed decrease of incorporated magnetic nanoparticles followed an exponential decay, and reached a near-steady state for incubation times longer than 1 hour.
Abbreviation: NP, nanoparticles.

The effects of the abovementioned treatments on cell viability were evaluated using several criteria, including direct observation of cell motility using optical microscopic observation, mitochondrial activity using an MTT assay, and detailed morphology using scanning electronic microscopy (SEM). Qualitative observation of the samples examined using the previously described treatments showed that the MNPs^{+}/TVMF^{+} population caused 100% cell death (see Supplementary materials). Quantitative analysis of the cells by MTT assay revealed that the cell viability of all of the other samples was not affected compared with the control (MNPs^{-}/TVMF^{-}, Figure 3). Analysis of all four samples using SEM revealed severe structural damage in cell morphology only for the MNPs^{+}/TVMF^{+} population, particularly at the level of the cell surface, indicating severe plasma membrane damage (Figure 4).

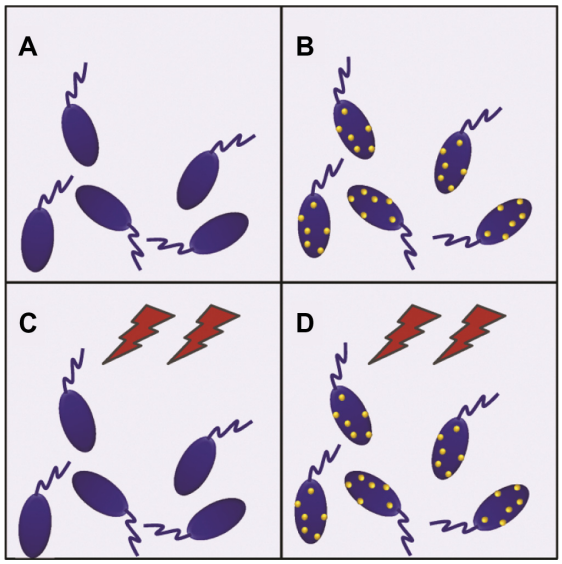

Figure 2 Schematic view of the experimental 2 × 2 design for evaluating the effect of magnetic nanoparticles and time-varying magnetic fields on *Crithidia fasciculata*. (**A**) Cells without magnetic nanoparticles not submitted to magnetic fields. (**B**) Cells with magnetic nanoparticles without magnetic field application. (**C**) Application of magnetic fields on unloaded cells. (**D**) Application of magnetic fields on magnetic nanoparticle-loaded cells.

Cell death

Because application of the TVMFs was performed in an adiabatic device, hyperthermia treatment could have produced a transient macroscopic increase in the sample temperature due to differences in rates of heat generation and dissipation. When a positive control experiment was conducted by applying a TVMF to a suspension containing only MNPs (Figure 5), the sample showed a large increase in temperature of about 50°C over the 30 minutes of the experiment. Therefore, we tested whether a similar increase in average temperature might have contributed to the amount of cell death by monitoring the temperature of the extracellular medium during application of TVMF. The results for both the controls and magnetically loaded cells showed only a slight macroscopic increase in temperature (about 2°C–4°C) after 30 minutes of TVMF application. This result (ie, an absence of temperature increase in samples composed of magnetically loaded cells) is expected, based on the much lower "average concentration" of MNPs in these samples, because the small amounts of uploaded MNPs are contained within a total volume of about 0.5 mL of liquid cell medium.

These results clearly demonstrate that the heat released from the MNPs was not enough to increase the average

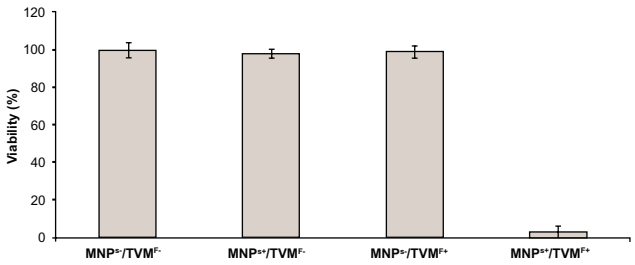

Figure 3 MTT assay results for the four conditions displayed in Figure 2.
Notes: All samples showed 100% of cell viability except in the case of time-varying magnetic fields applied on magnetically loaded cells, which caused 95% ± 5% cell death.
Abbreviations: MNPs^{-}/TVMF^{-}, cells not-bearing MNPs that were not submitted to TVMF; MNPs^{+}/TVMF^{-}, cells bearing MNPs that were not submitted to magnetic field application; MNPs^{-}/TVMF^{+}, cells not bearing MNPs that were submitted to magnetic field application; MNPs^{+}/TVMF^{+}, cells bearing MNPs that were submitted to magnetic field application; MNPs, magnetic nanoparticles; TVMF, time-varying magnetic field; MTT, (3-(4,5-Dimethylthiazol-2-yl)-2,5-diphenyltetrazolium bromide.

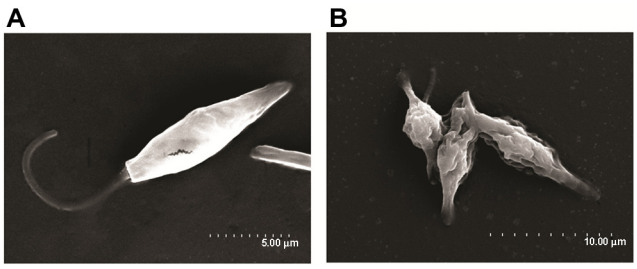

Figure 4 Scanning electron microscopy images of MNPs$^+$ (magnetic nanoparticles)/TVMF$^+$ (time-varying magnetic field) sample before (**A**) and after (**B**) application of magnetic fields.
Note: In the latter case, the changes in cell morphology can be clearly observed, reflecting the severe cell damage after TVMF.

temperature of the cell culture in such a way that would compromise viability of the cells. Therefore, the origin of cell death measured after application of TVMF should not be related to thermal stress. This is in agreement with previous works on magnetically loaded human dendritic cells,[19,28] demonstrating that application of TVMF for 30 minutes yielded up to 90%–95% cell death, without affecting blank cells without MNPs. Similar results have been reported in an HeLa cell line[29] loaded with MNPs. Some theoretical models of metal nanoparticles have also suggested this possibility.[30] Because the temperature was essentially constant during the experiments, the cell death observed suggests an intracellular MNP-triggered mechanism different from the apoptosis induced by hyperthermia. However, because the temperature was measured with a macroscopic sensor, the possibility of intracellular heating up to apoptotic temperatures cannot be excluded.

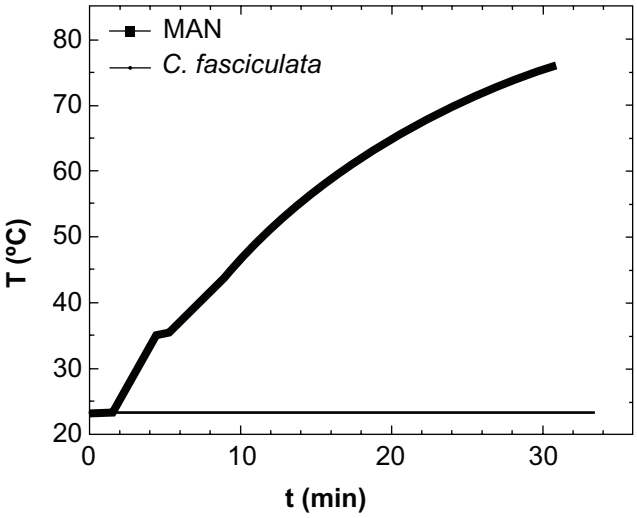

Figure 5 Specific power absorption of magnetic colloid (solid squares) at 1% weight concentration, and the nanoparticle-loaded protozoa (solid line) during application of AC magnetic field (H = 160 Oe, f = 250 kHz).
Abbreviations: MAN, magnetic colloid; *C. fasciculata*, *Crithidia fasciculata*; T, temperature; t, time.

To evaluate the plausibility of intracellular heating during our experiments, a simplified heat transfer model at the single-cell level was considered, eg, a single cell magnetically loaded with MNPs, surrounded by a large matrix of unloaded cells (or culture medium free of MNPs). We estimated the expected intracellular temperature increase in such a case based on the measured mass of MNPs in the intracellular medium, the calculated average cell volume from SEM images (230 ± 50 µm^3), and the measured specific power absorption values of the pure magnetic colloid. For simplicity, we further approximated the specific heat capacity of a single cell to the pure water value of $C_p = 4.18$ J/(g · K). From the average cell volume and MNP upload (1–10 pg/cell), we estimated a temperature increase rate of 0.02–0.87 K/sec. The above calculations were made considering that no heat was dissipated from the intracellular medium to the cell environment, which was a clearly unrealistic hypothesis. Because the cell membrane has non-negligible thermal conductivity, the calculated heating rates were not enough to increase the intracellular temperature up to the 41°C–45°C needed for triggering thermally induced apoptotic mechanisms.

Several prior studies suggest that apoptosis-related mechanisms are a main cause of hyperthermia-associated cell death.[19,31] Apoptosis (cellular programmed death) is a precise mechanism in which cells follow a programmed sequence of events to induce their death, with minimal disturbance to the total cell population.[32] This phenomenon appears to be present in a wide range of organisms, from primitive single-cell to higher multicellular eukaryotes. In the present work, we investigated whether the cell death of *C. fasciculata* induced by magnetic hyperthermia was attributable to apoptosis. An early event considered to be a marker of apoptosis is the appearance of phosphatidylserine on the external surface of the plasma membrane. Cells that incorporated nanoparticles and controls that were either submitted or not submitted to the magnetic field were incubated with annexin (used to detect the presence of phosphatidylserine) and propidium iodide (used to detect damage to the plasma membrane). Next, the four populations of cells were analyzed using flow cytometry. As illustrated in Figure 6, the results confirm 100% viability for MNPs$^-$/TVMF$^-$, MNPs$^+$/TVMF$^-$, and MNPs$^-$/TVMF$^+$ cell samples and 0% viability of MNPs$^+$/TVMF$^+$ cells. In this last case, it was observed that the cells were reactive to annexin and permeable to propidium iodide, indicating plasma membrane damage, which was confirmed using SEM (Figure 4). These results suggest that application

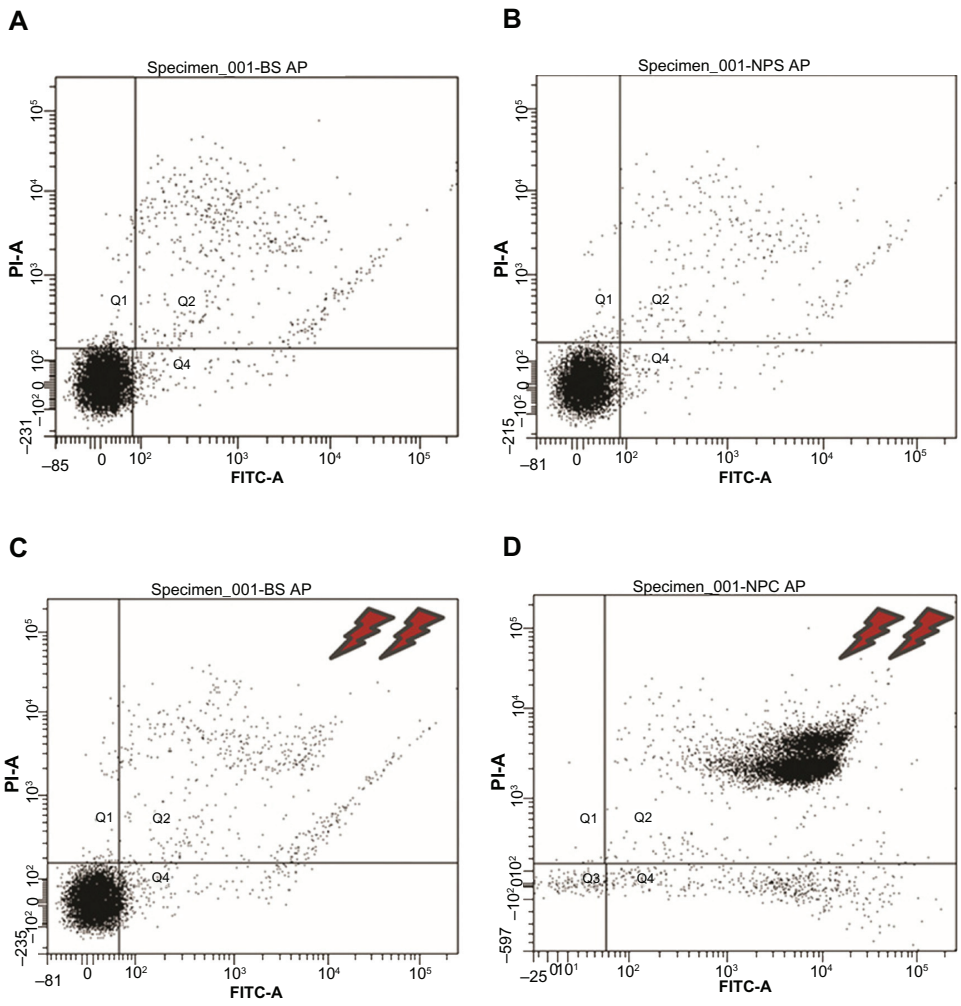

Figure 6 Flow cytometry results of the 2 × 2 experiments shown in Figure 2 (see text for details). Experiments (**A**–**C**) showed 89%–91% cell viability, whereas for experiment (**D**), application of magnetic fields for 30 minutes on magnetically charged cells resulted in only 9% cell survival.
Abbreviations: PI-A, propidium iodide; FITC, fluorescein isothiocyanate.

of TVMF to cells incorporating MNPs results in cell death via a nonapoptotic mechanism. Recent work on application of TVMF in magnetically loaded cells showed that a large decrease in cell viability can be achieved without an actual temperature increase in the cell medium.[29,33] Furthermore, it has been reported that, in the case of magnetically loaded dendritic cells, the percentage of cell death was proportional to the amount of MNPs taken up.[34] Because the cell death observed in our work corresponds to the maximum amount of uploaded MNPs (ie, after 15 minutes of cocultivation), it is still to be determined whether a similar effect could be achieved with smaller amounts of uploaded MNPs.

Taken together, our results lead us to propose that, in this case, irreversible cell injury due to mechanical stress (evidenced by SEM) in $MNPs^{+}$/$TVMF^{+}$ cell samples is the main cause of death. Theoretical calculations on the effect of the power released by MNPs on the cell membrane supports this hypothesis.[35] However, it is worth mentioning that other factors, such as liberation of toxic proteins into the cytoplasm due to disruption of membranes compartmentalizing them inside specific organelles like lysosomes, cannot be ruled out as simultaneous cause of cell injury and death.

Conclusion

In conclusion, the series of experiments reported here demonstrated as a proof of principle that magnetically induced hyperthermia can cause death of micro-organisms. Our results also illustrate that hyperthermia is a thermal phenomenon at a subcellular level because no macroscopic increase of temperature was observed. We were able to show that hyperthermia was specific for cells incorporating MNPs and submitted to TVMF because neither the nanoparticles nor TVMF alone resulted in loss of viability. Lastly, cells submitted to the hyperthermia treatment were dramatically damaged at the

plasma membrane level. It should be stressed that although this methodology is being extensively investigated and is currently used for mammalian cells, to our knowledge, it is not currently being proposed to treat diseases caused by micro-organisms. The present study highlights this method as a potential and novel alternative to treat infections caused by micro-organisms. A major advantage of this method is that it causes selective physical damage to target cells. Therefore, the probability of emergence of resistant strains is small. More detailed studies are also being conducted to identify the mechanisms involved in cell death in greater detail. Developing delivery systems with the capability to direct MNPs specifically to infectious agents remains a challenge. These findings lead us to propose this method as a novel strategy for developing new therapeutics against pathogenic micro-organisms.

Acknowledgments

This work was supported by the Spanish Ministry Ministerio de Ciencia e Innovación (project MAT2010-19326 and Consolider NANOBIOMED CS-27 2006) and IBERCAJA. Partial support from Brazilian grants 08/57596-4 and 11/50631-1 from FAPESP and INBEQMeDI, respectively, is also acknowledged. We gratefully recognize Doctors M Vergés, MP Morales, and AG Roca for their kind donation of MNPs. We also thank J Godino from the Instituto Aragonés de Ciencias de la Salud, Zaragoza, for help with flow cytometer measurements, and I Echaniz for technical support, and L Casado for help with scanning electron microscopy imaging.

Disclosure

The authors report no conflicts of interest in this work.

References

1. Rascalou G, Pontier D, Menu F, Gourbiere S. Emergence and prevalence of human vector-borne diseases in sink vector populations. *PloS One*. 2012;7:e36858.
2. Hotez PJ, Molyneux DH, Fenwick A, et al. Control of neglected tropical diseases. *N Engl J Med*. 2007;357:1018–1027.
3. Goya GF, Fernandez-Pacheco R, Arruebo M, Cassinelli N, Ibarra MR. Brownian rotational relaxation and power absorption in magnetite nanoparticles. *J Magn Magn Mater*. 2007;316:132–135.
4. Lacroix LM, Malaki RB, Carrey J, et al. Magnetic hyperthermia in single-domain monodisperse FeCo nanoparticles: evidences for Stoner-Wohlfarth behavior and large losses. *J Appl Phys*. 2009;105(2).
5. Santos DM, Carneiro MW, de Moura TR, et al. Towards development of novel immunization strategies against leishmaniasis using PLGA nanoparticles loaded with kinetoplastid membrane protein-11. *Int J Nanomedicine*. 2012;7:2115–2127.
6. Danesh-Bahreini MA, Shokri J, Samiei A, Kamali-Sarvestani E, Barzegar-Jalali M, Mohammadi-Samani S. Nanovaccine for leishmaniasis: preparation of chitosan nanoparticles containing Leishmania superoxide dismutase and evaluation of its immunogenicity in BALB/c mice. *Int J Nanomedicine*. 2011;6:835–842.
7. Vyas SP, Gupta S. Optimizing efficacy of amphotericin B through nanomodification. *Int J Nanomedicine*. 2006;1:417–432.
8. Boscardin SB, Torrecilhas AC, Manarin R, et al. Chagas' disease: an update on immune mechanisms and therapeutic strategies. *J Cell Mol Med*. 2010;14:1373–1384.
9. Pinto Dias JC. The treatment of Chagas disease (South American trypanosomiasis). *Ann Intern Med*. 2006;144:772–774.
10. Filardi LS, Brener Z. Susceptibility and natural resistance of *Trypanosoma cruzi* strains to drugs used clinically in Chagas disease. *Trans R Soc Trop Med Hyg*. 1987;81:755–759.
11. Wilkinson SR, Kelly JM. Trypanocidal drugs: mechanisms, resistance and new targets. *Expert Rev Mol Med*. 2009;11:e31.
12. Pepin J, Milord F, Khonde A, Niyonsenga T, Loko L, Mpia B. Gambiense trypanosomiasis: frequency of, and risk factors for, failure of melarsoprol therapy. *Trans R Soc Trop Med Hyg*. 1994;88:447–452.
13. Goto H, Lindoso JA. Current diagnosis and treatment of cutaneous and mucocutaneous leishmaniasis. *Expert Rev Anti Infect Ther*. 2010;8:419–433.
14. Berman JD. Human leishmaniasis: clinical, diagnostic, and chemotherapeutic developments in the last 10 years. *Clin Infect Dis*. 1997;24:684–703.
15. Berman JD. US Food and Drug Administration approval of AmBisome (liposomal amphotericin B) for treatment of visceral leishmaniasis. *Clin Infect Dis*. 1999;28:49–51.
16. Jordan A, Wust P, Fahling H, John W, Hinz A, Felix R. Inductive heating of ferrimagnetic particles and magnetic fluids: Physical evaluation of their potential for hyperthermia. *Int J Hyperthermia*. 2009;25:499–511.
17. Goya GF, Grazu V, Ibarra MR. Magnetic nanoparticles for cancer therapy. *Curr Nanosci*. 008;4:1–16.
18. Lee J-H, Jang J-T, Choi J-S, et al. Exchange-coupled magnetic nanoparticles for efficient heat induction. *Nat Nanotechnol*. 2011;6:418–422.
19. Levy M, Wilhelm C, Siaugue JM, Horner O, Bacri JC, Gazeau F. Magnetically induced hyperthermia: size-dependent heating power of gamma-Fe(2)O(3) nanoparticles. *J Phys Condens Matter*. 2008;20:204133.
20. Comini M, Menge U, Wissing J, Flohe L. Trypanothione synthesis in *Crithidia* revisited. *J Biol Chem*. 2005;280:6850–6860.
21. Verges MA, Costo R, Roca AG, et al. Uniform and water stable magnetite nanoparticles with diameters around the monodomain-multidomain limit. *J Phys D Appl Phys*. 2008;41(13).
22. Gonzalez-Fernandez MA, Torres TE, Andres-Verges M, et al. Magnetic nanoparticles for power absorption: optimizing size, shape and magnetic properties. *J Solid State Chem*. 2009;182:2779–2784.
23. Goya GF. Handling the particle size and distribution of Fe3O4 nanoparticles through ball milling. *Solid State Commun*. 2004;130:783–787.
24. Hergt R, Dutz S, Roder M. Effects of size distribution on hysteresis losses of magnetic nanoparticles for hyperthermia. *J Phys Condens Matter*. 2008;20:385214.
25. Hilger I, Fruhauf K, Andra W, Hiergeist R, Hergt R, Kaiser WA. Heating potential of iron oxides for therapeutic purposes in interventional radiology. *Acad Radiol*. 2002;9:198–202.
26. Pineiro-Redondo Y, Banobre-Lopez M, Pardinas-Blanco I, Goya G, Lopez-Quintela MA, Rivas J. The influence of colloidal parameters on the specific power absorption of PAA-coated magnetite nanoparticles. *Nanoscale Res Lett*. 2011;6:383.
27. Goya GF, Marcos-Campos I, Fernandez-Pacheco R, et al. Dendritic cell uptake of iron-based magnetic nanoparticles. *Cell Biol Int*. 2008;32:1001–1005.
28. Marcos-Campos I, Asin L, Torres TE, et al. Cell death induced by the application of alternating magnetic fields to nanoparticle-loaded dendritic cells. *Nanotechnology*. 2011;22:205101.
29. Villanueva A, de la Presa P, Alonso JM, et al. Hyperthermia HeLa cell treatment with silica-coated manganese oxide nanoparticles. *J Phys Chem C*. 2010;114:1976–1981.

30. Richardson HH, Carlson MT, Tandler PJ, Hernandez P, Govorov AO. Experimental and theoretical studies of light-to-heat conversion and collective heating effects in metal nanoparticle solutions. *Nano Lett*. 2009;9:1139–1146.
31. Schildkopf P, Frey B, Mantel F, et al. Application of hyperthermia in addition to ionizing irradiation fosters necrotic cell death and HMGB1 release of colorectal tumor cells. *Biochem Biophys Res Commun*. 2010;391:1014–1020.
32. Peter ME. Programmed cell death: apoptosis meets necrosis. *Nature*. 2011;471:310–312.
33. Creixell M, Bohorquez AC, Torres-Lugo M, Rinaldi C. EGFR-targeted magnetic nanoparticle heaters kill cancer cells without a perceptible temperature rise. *ACS Nano*. 2011;5:7124–7129.
34. Asín L, Ibarra M, Tres A, Goya GF. Controlled cell death by magnetic hyperthermia: effects of exposure time, field amplitude, and nanoparticle concentration. *Pharm Res*. 2012;29(5):1319–1327.
35. Lunov O, Zablotskii V, Pastor JM, et al. Thermal destruction on the nanoscale: cell membrane hyperthermia with functionalized magnetic nanoparticles. In: Hafeli U, Schutt W, Zborowski M, editors. *8th International Conference on the Scientific and Clinical Applications of Magnetic Carriers*. Vol 1311. Melville, NY: Amer Inst Physics; 2010.

Supplementary materials

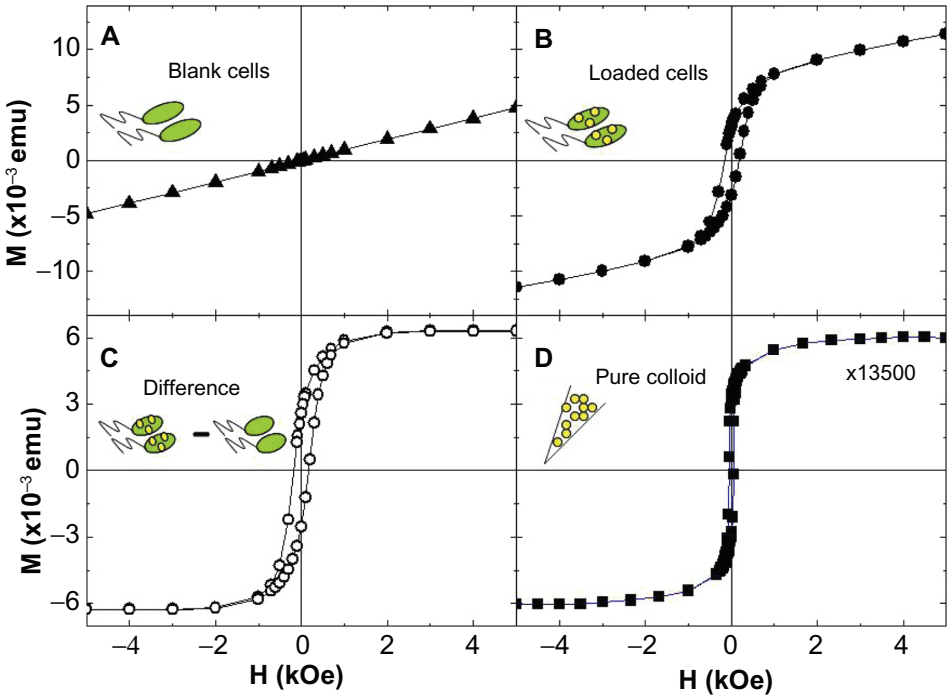

Figure S1 Magnetic response at T = 10 K from (**A**) unloaded cells, (**B**) response from *Crithidia fasciculata* cocultured with MNPs (sample incubated for 15 minutes), (**C**) difference between loaded and unloaded cells (B – A), and (**D**) pure magnetic colloid. Note that for the pure colloid (D), the curve was divided by 1.35×10^4 to fit the same scale as the magnetic signal from loaded cells (C).

Notes: To calculate the amount of magnetic material m_{mag} incorporated by the cells, the M_S values from the pure colloids and from the magnetic nanoparticle-loaded cells were calculated as m_{mag} [g/cell] = M/MS × *Number of cells.* The number of magnetic nanoparticles per single cell was estimated from the known average particle diameter.

The 2 × 2 design for evaluating the effect of magnetic nanoparticles and time-varying magnetic fields on *Crithidia fasciculata*

- File "a.mov": Cells without magnetic nanoparticles not submitted to magnetic fields
- File "b.mov": Cells with magnetic nanoparticles without magnetic field application
- File "c.mov": Application of magnetic fields on unloaded cells
- File "d.mov": Application of magnetic fields on magnetic nanoparticle-loaded cells